CrossMark

ORIGINAL ARTICLE

Investigation of effects of cutting insert rake face forms on surface integrity

Hüseyin Gürbüz[1] · Ulvi Şeker[2] · Fırat Kafkas[2]

Abstract In this study, the effects of cutting insert rake face forms and cutting parameters on the surface integrity in machining of AISI 316 L steel were investigated experimentally. The cutting forces occur during chip removal, surface roughness values on the machined surfaces with residual stresses on machined workpiece were measured, and metallurgical structure (microhardness and microstructural variations) of the surface layers formed as a result of machining were evaluated. The surface integrity was evaluated in terms of surface roughness, residual stress, microhardness, and microstructure analysis. In experiments, the best surface integrity results were obtained by cutting tools having QM form, and the worst surface integrity results were obtained by cutting tools having MR form. Under all these cutting conditions, it was observed that the surface integrity worsened when depth of cut and cutting feed were increased; however, the surface integrity improved when cutting speed was increased. In terms of cutting parameters, the best surface integrity was obtained with cutting speed 200 m/min, cutting feed 0.1 mm/rev, and depth of cut 1.25 mm; on the other hand, the worst surface integrity was obtained with cutting speed 125 m/min, cutting feed 0.3 mm/rev, and depth of cut 2.5 mm.

✉ Hüseyin Gürbüz
huseyin.gurbuz@batman.edu.tr

Ulvi Şeker
useker@gazi.edu.tr

Fırat Kafkas
fkafkas@gazi.edu.tr

[1] Faculty of Technology, Batman University, Batman, Turkey

[2] Faculty of Technology, Teknikokullar, Gazi University, Ankara, Turkey

1 Introduction

The one of primary factor effecting chip formation in the process of chip removal is form of the tool rake face. Chip formation occurs by means of heat and stress taking place on primary deformation zone displaying changes with regard to form of the tool rake face (insert rake angle and length of the flat of rake face). Appropriate insert rake angle and length of the flat of rake face help the plastic deformation of metal to substantiate on a shorter shear plane, the tool/chip contact area to shorten, and the heat and power occurring in cutting area because of deformation to decline. Within this context, forms of cutting insert rake face provide a positive effect on surface integrity of machined workpieces by helping to decrease the thermal and mechanical effects having a significant influence on residual stresses, microhardness, and microstructural changes induced by plastic deformation.

Surface integrity has three components. First of these is surface texture, meaning surface roughness (for instance, surface finish, dimensional, and form accuracy); the second one is metallurgical structure of surface layers having occurred after machining (microhardness, microstructural changes); and the last one is the residual stresses having occurred on the surface and sub-surface areas [1]. Machining process is significantly characterized by high stresses, high strain ratio, high temperature, and generally within short interaction time (~0.1 ms) with workpiece during chip formation. Therefore, machining methods lead to microstructural alterations, microhardness changes, and residual stresses on the workpiece [2]. The result called as the surface integrity is crucial to finishing operations especially owing to part performance and harmony [2].

Springer

In order to evaluate the surface integrity having occurred as a result of metal cutting, numerous studies have been conducted [1–16]. The studies carried out showed that machining parameters and cutting tool properties affected the surface integrity of the workpiece generated as a result of chip removal. The materials used in these studies performed are American Iron and Steel Institute (AISI) 304 stainless steel [3], titanium alloys [4, 5], Inconel 718 [1, 6, 7], CoCrMo alloy [8], B8 bainitic steel [12, 13], and AISI 52100 [14, 16]. However, surface integrity studies about AISI 316 L austenitic stainless steel have not been encountered. Publications mentioned above about surface integrity are briefly given below. Alexander et al. investigated the effects of cutting parameters on surface integrity occurring turning of AISI 304 stainless steel. In the study, they found out that cutting feed affected surface roughness most and an almost 60–70-μm work hardened layer occurred beneath the machined surfaces [3]. Che-Haron examined surface integrity and cutting tool life in turning of titanium alloys. He obtained a very thin layer immediately beneath the machined surface with regard to plastic deformation influenced and the highest microhardness value beneath the machined surface, where the microstructures were heavily deformed [4]. Later, Che-Haron and Jawaid investigated the effect of machining conditions on surface integrity of Ti–6 % Al–4 % V titanium alloy. In the study, they determined that there was a deformed area beneath the machined surface and that a work hardening occurred beneath the machined surface depending upon plastic deformation [5]. Devillez et al. investigated surface integrity of Inconel 718 depending on dry and cooling liquid and change in cutting speed. In the light of the results they obtained, they put forward that depending on change in cutting speed, residual stress and microhardness values dropped when cooling liquid was used and at the same time, the area affected by deformation was less [6]. Arunachalam et al. investigated the effect of coated cutting tools on surface integrity of Inconel 718. In the results, they determined that cutting tool properties were dominant in determination of residual stress profile [1]. Sharman et al. examined the effect of cutting tool nose radius on residual stress and surface integrity in turning Inconel 718. The results demonstrated that microstructure deformation depth increased when cutting tool nose radius increased, and that tensile residual stresses were obtained close to the place of machined surface [7]. Bordin et al. investigated the effect of cutting speed and cutting feed on surface integrity in dry turning of CoCrMo alloy. In the study they performed, they found out that cutting feed and cutting speed had a significant effect on surface integrity [8]. Jacobson et al. dealt with how cutting speed affected the surface integrity of hard-turning bainitic steel. The results showed that cutting speed affected residual stresses and surface roughness. They emphasized that compressive residual stresses they obtained were values to have positive effect on fatigue life. Moreover, they mentioned that microstructure in surface and sub-surface areas changed either very little or none [9].

Rech and Moisan investigated the effect of cutting parameters and tool wear on surface integrity (surface roughness and residual stresses) in turning of cementation steels. The authors emphasized that when workpieces were machined at low cutting feed and low cutting speeds, this caused compressive residual stresses and low surface roughness values [10]. Matsumoto et al. searched the effect of hard turning on surface integrity. With this study, they found out that hard workpiece turning had an effect on fatigue life since it produced compressive residual stresses. Moreover, they examined the effect of machining parameters and cutting tool edge geometry on residual stresses and determined that cutting tool edge geometry dominated more in determining residual stress profile [11]. El-Wardany et al. investigated the effect of cutting conditions and tool wear on surface integrity and chip morphology occurring during the machining of AISI D2 tool steel at high cutting speeds. When machining was carried out by means of a sharp cutting tool, they established that the layer thickness in the area affected by heat inside surface was a lot less compared to a worn tool. Besides, they observed a lower microstructure alteration at 10–15-μm depth immediately beneath machined surface [12]. Kishaways and Elbestatwi, on the other hand, examined surface integrity and wear characteristics during high-speed turning of AISI D2 tool steel. They determined that machined surface and sub-surface errors and residual stress distributions depended on cutting parameters and prepared various cutting edges [13]. In their study, Schwach and Gou found out optimal surface integrity with affecting parameters on surface integrity in turning AISI 52100 components [14]. Afterward, Smith et al. investigated the effect of surface integrity on fatigue performance of AISI 52100 in hard turning. When all surface integrity experiments are examined, it can be seen that the authors emphasize that compressive residual stresses lead to the most significant influence on fatigue life [15]. However, Shi and Liu tried to develop fatigue life and surface integrity by removing rough and fine chips from AISI 52100 steel [16].

As a result of the review of the literature, studies in which the effects of cutting insert rake face forms and cutting parameters on surface integrity in machining AISI 316 L austenitic stainless steel are handled as a whole have not been encountered. The experimental studies conducted demonstrated that the workpiece machined as a result of chip removal affected surface integrity with regard to various parameters. However, there are still a number of questions related with the issue in order to determine the surface integrity occurring after machining and to obtain the required surface integrity and to find out the properties and reasons effecting surface integrity. For all these reasons, this experimental study has the properties to fill a gap since it presents different features to the literature [17, 18].

2 Experimental studies

It was pointed out by Astakhov and Xiao [19] that the shape of the rake face of indexable cutting insert can have significant influence on the metal-cutting process. This is because that not only the rake angle but also the shape of the rake face affects the state of stress, and thus stress triaxiality, in the deformation zone. As a result, by altering this shape, one can minimize the energy spent in the cutting process and thus decrease the cutting force and improve the integrity of the machined surface. Astakhov and Xiao, however, showed this numerically and verified the results only in orthogonal cutting tests with a simple-shaped cutting insert. This paper aims to carry out a test program with commercial cutting inserts in attempt to verify the proposed approach in real-life cutting. The tests aim to show that the shape of the real inserts and parameters of machining regime significantly affect the cutting force and machined surface integrity and thus cutting performance.

3 Material and methods

3.1 Workpiece material, cutting tools, and tool holder

AISI 316 L austenitic stainless steel is used as workpiece material in the experiments. The unmachined experimental material is of Ø 25 × 125-mm dimensions. The chemical composition of it is given in Table 1. In the experimental studies, cementite carbide-cutting tools in the form of SNMG and tool holders in the form of PSBNR 2525 M12 having 75° approaching angle for cutting tools were used [20]. The scheme showing input parameters was used in experimental studies with examined outputs in Fig. 1.

Appropriate for workpiece material, GC2025 grades, covered by CVD [(three-layer TIN-Al$_2$O$_3$-Ti (C, N)] of SANDVIK company equivalent to ISO M25 grade, were chosen. For cutting tools, cutting tools with the form of SNMG 120408 MR/MM/QM of SANDVIK tool manufacturing company were determined [21]. These cutting tools were chosen to determine the effect of cutting insert rake face forms (insert rake angle and length of the flat portion of the rake face) on the surface integrity of AISI 316 L workpiece apart from cutting parameters (cutting speed, cutting feed, and cutting depth) during machining.

Table 1 The chemical composition of workpiece material

%C	%Mn	%Si	%S	%P	%Ni
0.023	1.27	0.44	0.021	0.034	10.10
%Cr	%Mo	%Cu	%N	%Co	
16.17	2.13	0.45	0.043	0.16	

3.2 Cutting parameters and machining tests

The cutting parameters, four different cutting speeds (125, 150, 175, and 200 m/min), three different cutting feeds (0.1–0.2–0.3 mm/dev), and two different depths of cut (1.25 and 2.5 mm), were chosen by taking the tool manufacturing companies' data and suggestions of ISO 3685 into consideration. In experiments, measurement was carried out by machining the samples. In machining AISI 316 L steel, in order to figure out its effect on surface integrity, the geometrical features of cutting tools used and cutting parameters are given in Table 2.

3.3 Machine tool, cutting forces, and surface roughness measuring

The experiments were carried out on TC-35 JOHNFORD CNC turning lathe having FANUC control unit. Cutting forces were measured by KISTLER 9275B type dynamometer. So as to measure surface roughness of the machined workpieces, Mahr Perthometer M1 measurement device with serial number 9633 was used. For surface roughness values, measurements from randomly peripherally selected 10 different points on the surface of machined workpiece with sampling length of 5.6 mm were obtained and their arithmetical means were taken.

3.4 Measurement and detection of residual stresses

In order to measure residual stresses occurring on the machined workpieces, X-ray diffraction measurement device (SEIFERT XRD 3003 PTS) was used. By employing $\sin^2 \psi$ method in determining residual stresses, it was measured with the help of X-ray diffraction technique. Residual stresses were measured taking three measurements from each machined surface. Taking the residual stress value means (both circumferential and axial direction) from the measured workpiece, graphics were created. The depth of residual stress profiles occurring as a result of machining was taken at the length of 5 μm from the surface of each workpiece. Parameters used in X-ray analyses were given in Table 3 for AISI 316 L workpiece.

3.5 Microhardness measurements and analysis of microstructure

SHIMADZU HMV2 model microhardness device was used so that hardness having occurred on the samples with chip removal process could be measured. Microhardness experiments were conducted via Vickers hardness measurement method beneath a load of 0.5 kgf (4903 N) and being kept waiting for 5 s. Microhardness measurements were taken as arithmetical means measuring at three different points, in the form to make 120° peripherally until 1.4-mm depth with

Fig. 1 The scheme showing input parameters used in experimental studies with examined outputs
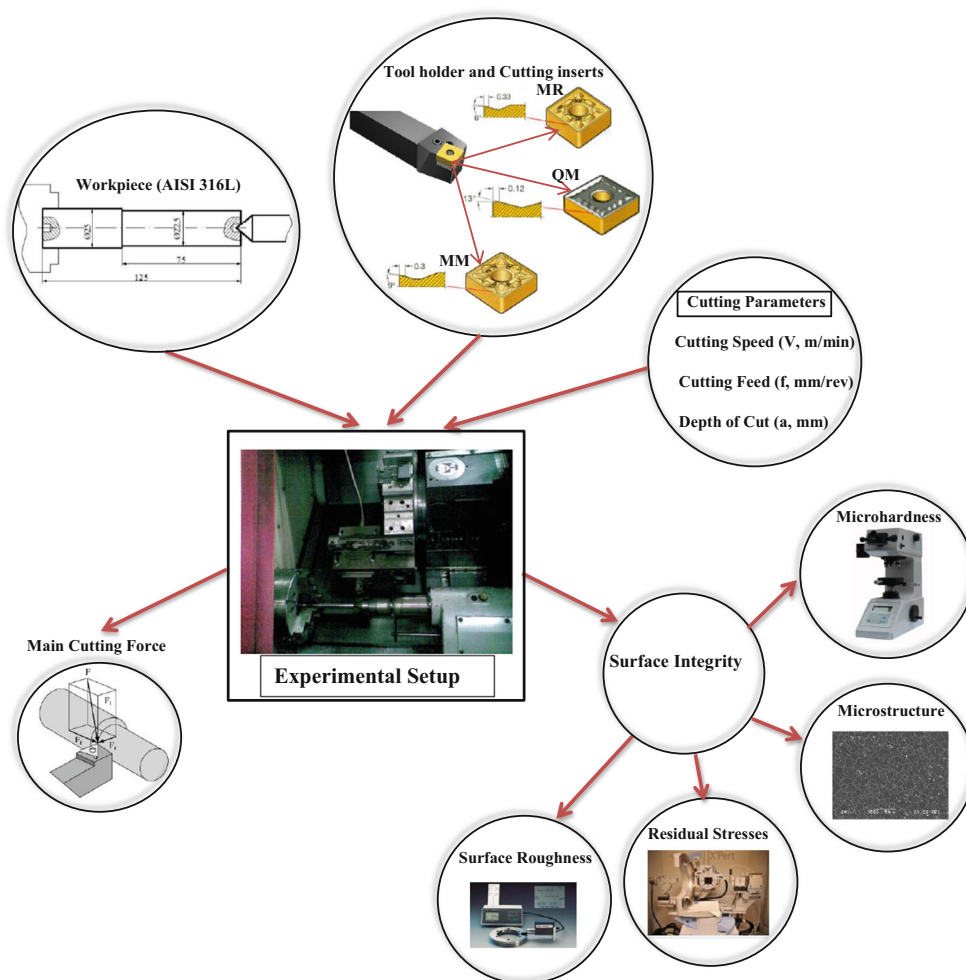
gradual increases of 0.1 from the machined edge of each surface toward the raw material (to the center of workpiece). As a result of machining, occurring microstructural characterization studies were carried out by means of *JEOL JSM 6060LV* model scanning electron microscope (SEM).
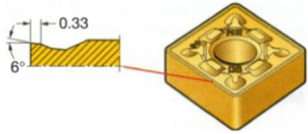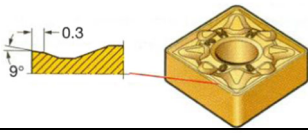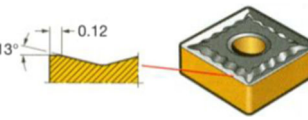
4 Experimental results and discussion

4.1 Evaluation of cutting forces

The changes in cutting forces are shown in Fig. 2 depending on forms of cutting insert rake face and cutting parameters. When the graphics in Fig. 2 is inspected, it can be said that cutting forces increase with the increase of cutting feed and depth of cut but decrease with the increase of cutting speed. The appearing case is the same for three different cutting tool forms. This situation is in good agreement with the literature [27–29]. The decrease in cutting forces with increasing cutting speed was explained with decrease in tool/chip contact area and partial decrease in shear strength in flow zone (secondary deformation zone) due to rise in temperature [29, 30]. With increase in

cutting feed and depth of cut, increase in cutting forces is an expected case. The effect of depth of cut on cutting forces is the probable reason that when the depth of cut increases, the volume of the uncut chip also increases, which produces more resistance on the cutting tool, and the material removal rate increases, which contributes to increase in cutting forces [31]. When the cutting feed increase, it can be attributed to increases in the friction and contact area between cutting tool and workpiece, which in turn increases the cutting forces, and therefore, cutting forces increase as the cutting feed increases [31, 32].

When cutting force graphics in Fig. 2 are examined, it will be observed that the highest cutting forces are obtained with cutting tools having MR-MM-QM forms, respectively. The energy used during chip removal arises as shear energy in primary deformation zone, in shear plane, and in shear and friction energy along the tool/chip contact [33]. As the rake angle increases, shear angle increases as well [34–36]. Small shear angle leads to increase in energy used for chip removal in cutting process by increasing the shear plane length in the primary deformation zone. Since there is shorter shear plane, as a result, large shear angle provides less energy to be spent for cutting process relatively [33]. Larger shear angle provides

Table 2 Geometrical features of cutting tools and cutting parameters used in experiments to determine their effects on surface integrity

Cutting Tool Geometry	Length of the flat portion of the rake face	Insert rake angles	Cutting Parameters		
			Cutting Speed (m/min)	Cutting feed (mm/rev)	Depth of cut (mm)
MR	0,33	6°			
MM	0,30	9°	125 150 175 200	0,1 0,2 0,3	1,25 2,5
QM	0,12	13°			

relatively less energy to be spent for cutting process since it contributes to shorter shear plane [33]. Therefore, while small rake angle increases cutting forces by decreasing shear plane angle, large rake angle, however, decreases the cutting forces by increasing shear plane angle. When insert rake angles of cutting tools used in experiments are evaluated in respect to their sizes, and when QM(13°)-MM(9°)-MR(6°) occurs, cutting forces lead to the formation by means of cutting tools with forms MR-MM-QM, respectively.

Also, it is known that tool/chip contact length has a significant effect on cutting forces. When cutting tools with MR-MM-QM form in Table 2 are inspected, it can be seen that, respectively, MR(0.33)-MM(0.30)-QM(0.12) possess the biggest

length of the flat of the rake face (the first flat where chip initially contacts with cutting tool edge). Bigger flat of the insert rake face increases tool/chip contact area, while smaller flat of the insert rake face decreases tool/chip contact area. Since this decreasing tool/chip contact length eases the flow of chip, this also helps the cutting forces decrease. Therefore, cutting tools having MR-MM-QM forms, respectively, are obtained for the highest cutting forces. In three different forms of the tool rake face, the lowest cutting forces were obtained when cutting speed was 200 m/min, cutting feed was 0.1 mm/rev, and depth of cut was 1.25 mm; on the other hand, the highest cutting forces were obtained when cutting speed was 125 m/min, cutting feed was 0.3 mm/rev, and depth of cut was 2.5 mm.

Table 3 Parameters used in X-ray analyses

Test material	Fe_γ	[22, 23, 24]
Spot area (mm^2)	1	[24]
$1/2S_2$ (MPa^{-1})	6531×10^{-6}	[24]
$-S_1$ (MPa^{-1})	1429×10^{-6}	[24]
Wavelength	Mn	[22, 23, 24, 25]
Radiation	K_α	[22, 23, 24, 25]
Filter	Cr	[22, 23, 24]
Bragg angle 2θ (deg)	128.70°	[26]
Lattice planes	(hkl) = (220)	[26]
Young's modulus (GPa)	196	[25]
Poisson's ratio	0.28	[25]

4.2 Evaluation of surface roughness

Average surface roughness values changes are given in Fig. 3 as graphics according to forms of cutting insert rake face and cutting parameters. When the graphics in Fig. 3 are inspected, it is seen that surface roughness tends to decrease depending on increase in cutting speed. The tendency that appears is the same for three different forms of the tool rake face. This tendency is expected. So as to better the surface roughness, increasing the cutting speed is the most common method in literature [37–39]. The researchers explained increase in cutting speed with decrease in surface roughness depending on increase in cutting speed with decrease in built-up edge (BUE) [30, 40, 41]. In the experiments carried out, it is observed that

Fig. 2 Effect of cutting insert rake face forms and cutting parameters on main cutting force Fc (N) **a** f = 0.1 mm/rev, **b** f = 0.2 mm/rev, and **c** f = 0.3 mm/rev
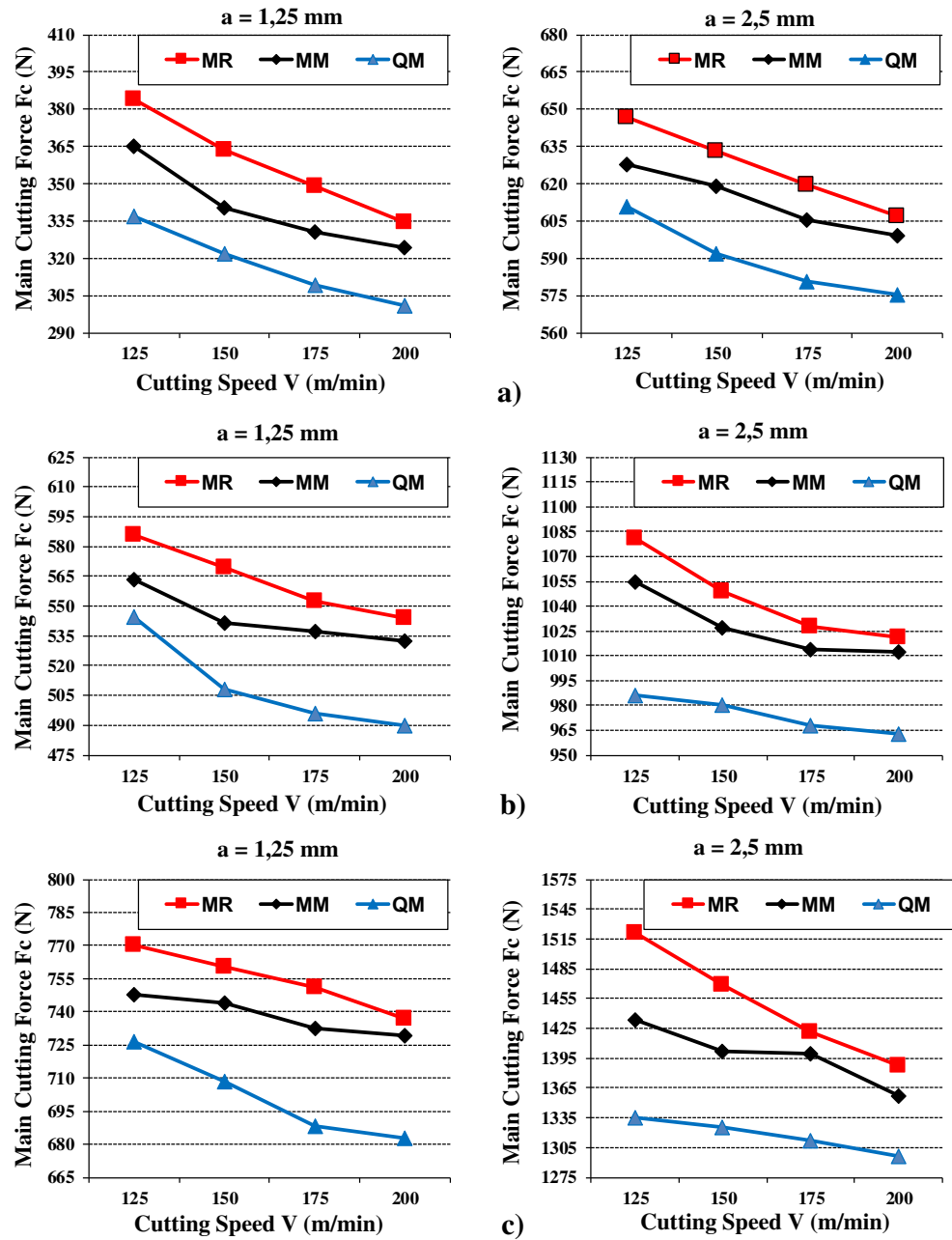

surface roughness increased depending on the increase in depth of cut (Fig. 3). Increase in surface roughness depending on the increase in depth of cut is attributed to increasing chip cross section. To evaluate the effect of cutting feed on surface roughness, when graphics in Fig. 3 are interpreted, surface roughness worsens as cutting feed is increased. In metal removal process, it is well known that increase in feed values causes bad surface roughness [42, 43], which is an expected case. During machining, the amount of heat generation increases with increase in cutting feed, which causes cutting tool wear, and in turn higher surface roughness [42, 43]. The increase in the cutting feed also increases the chatter, and this

produces incomplete machining at faster traverse, which leads to higher surface roughness [42].

The best surface roughness was obtained at 200-m/min cutting speed, 0.1-mm/rev cutting feed, and 1.25-mm depth of cut and with cutting tool having QM form; however, the worst surface roughness was obtained at 125-m/min cutting speed, 0.3-mm/rev cutting feed, and 2.5-mm depth of cut with cutting tool having MR form. When the surface roughness graphics in Fig. 3 are examined, the highest roughness values are obtained by means of cutting tools having MR (6°)-MM (9°)-QM (13°) insert rake angle, respectively. Under all cutting conditions in the experiments, the best surface quality was

Fig. 3 Effect of cutting insert rake face forms and cutting parameters on surface roughness Ra (μm) **a** f = 0.1 mm/rev, **b** f = 0.2 mm/rev, and **c** f = 0.3 mm/rev
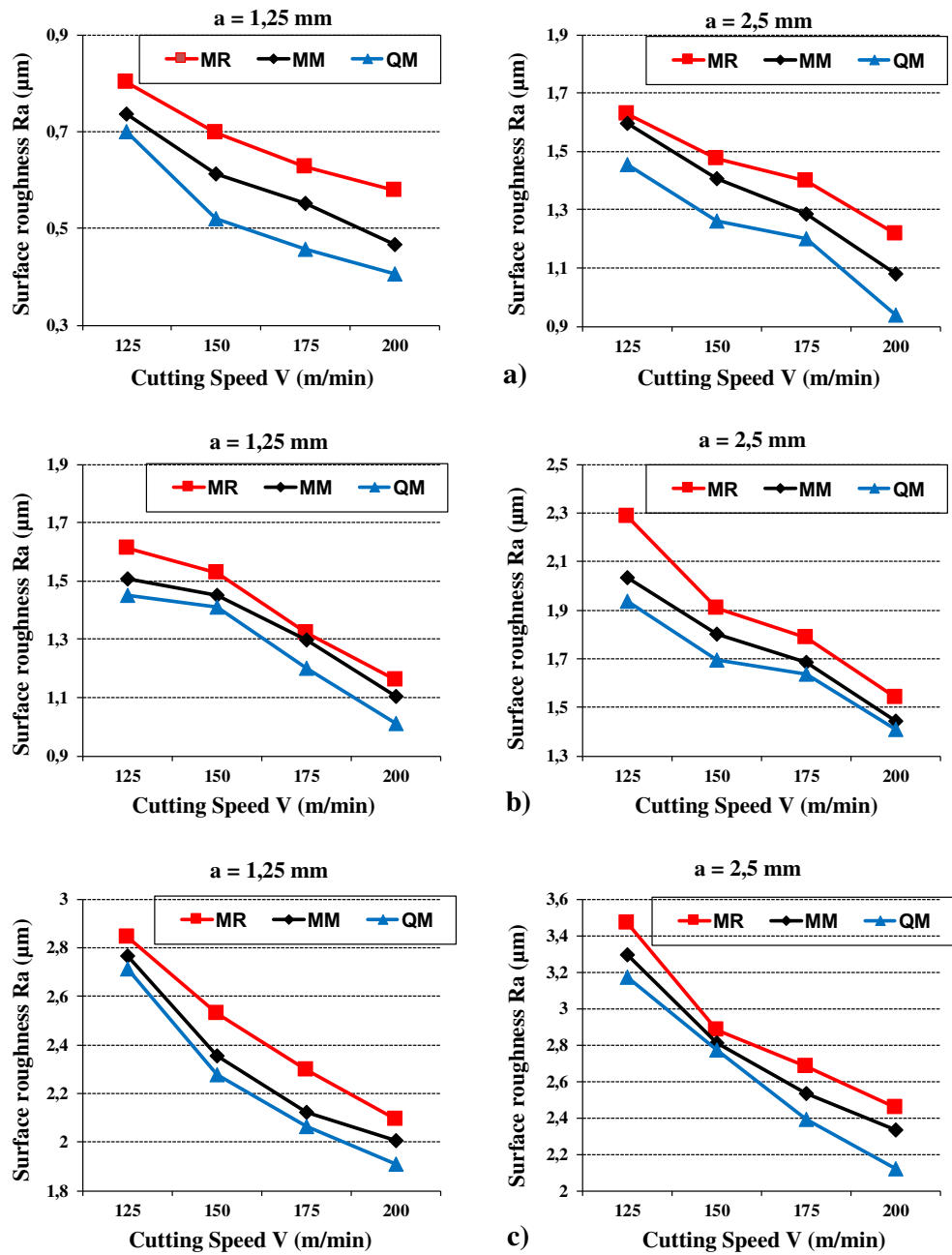
obtained from the surfaces machined by cutting tools having QM form and the worst surface quality was obtained from surfaces machined by cutting tools having MR form. The case in question was attributed that QM formed cutting tool with an insert rake angle of (13°) and MR formed cutting tool with an insert rake angle of (6°) (Table 2). It is known that as the rake angle increases, surface roughness values decrease and as the rake angle decreases, surface roughness values increase. Since BUE formation will decrease with the increase of rake angle and thus friction coefficient on rake surface of cutting tool will decrease, surface roughness values decrease [29].

Also, when cutting tools with MR-MM-QM forms as in Table 2, it is seen that MR(0.33)-MM(0.30)-QM(0.12) have

the largest flat of the insert rake face. While larger flat of the insert rake face increases the tool/rake contact area, smaller flat of the insert rake face decreases tool/rake contact area. Decreasing tool/chip contact length contributes to decrease the surface roughness values. Also, since the cutting tool with MR form is found suitable for rough cuttings by the manufacturing firm, a quality surface is not anticipated from such a cutting tool [21].

4.3 Residual stresses

While surface integrity is being evaluated, residual stress is considered to be one of the most critical parameters since it

has a direct impact on the fatigue life of the machined parts [44–47]. The studies of residual stress are particularly important to reach high reliability levels when critical structural components are machined [25, 48]. Residual stresses might have both positive and negative effects on the deformation behavior of machined parts, fatigue life, dynamic strength, chemical resistance, and magnetic properties [1, 6, 22, 48]. While compressive residual stresses usually enhance performance of workpiece and its life [1, 6, 14, 22, 44, 49], tensile residual stresses tend to reduce them [1, 6, 14, 49, 50]. The residual stresses created by machining operations can greatly affect the properties of austenitic stainless steels and their ability to withstand severe loading conditions (stress concentration, corrosion, cracking and fatigue) [23].

Austenitic stainless steels are considered to be difficult materials due to their low thermal conductivity, high tensile strength, high ductility, and high work hardening [23–25, 48, 51]. These properties often lead to high cutting forces and high cutting temperature, fast tool wear, difficulties with chip breakability, BUE formation, and poor surface finish [51]. This affects the surface integrity of the workpiece and leads to high residual stresses in the surface layers [48, 51]. In machining of austenitic stainless steels, there can especially be found tensile residual stresses in the circumferential direction (between 500 and 1000 MPa) at high values which influence the life of workpieces in a negative way [23, 24, 45, 48]. That is why it is important that residual stresses occur when machining materials such as austenitic stainless steels [51]. The residual stresses obtained in the experimental study carried out have been seen in the form of circumferential tensile residual stresses to reach up to about 750 MPa.

Residual stress values measured in the circumferential and axial directions of machined workpieces are shown in graphics in Figs. 4 and 5 depending on applied cutting parameters and forms of cutting insert rake face. When the values in graphics in Figs. 4 and 5 are examined, it is seen that for all machining experiments, the residual stresses obtained on the machined surface occur tensile residual stresses and the highest tensile residual stresses in circumferential direction and the lowest tensile residual stresses in axial direction. The same tendency was observed in previous studies [23, 48]. In experimental studies carried out, it is seen that generally when depth of cut and cutting feed increase, tensile residual stresses increase; on the other hand, with the increase in cutting speed, tensile residual stresses decrease (Figs. 4 and 5). The case which emerges is the same for three different cutting insert forms. As cutting speed increased, residual stresses decreased. In related previous studies, similar results emerged as well [24, 52, 53]. Because of the effect of cutting speed on the temperature in cutting area, this has a significant effect on residual stresses during machining [52]. Due to the high amount of energy consumption at high cutting speeds, more heat comes off. When cutting speed increased, although more

heat was formed, the amount of tensile residual stresses on machined surface decreased. Liu and Barash found similar results by obtaining high tensile residual stress at low cutting speeds during the machining of low carbonized steels [53]. Approximately 10–15 % of the heat occurring during machining are transferred to workpiece [53, 54]. When machining is carried out at high cutting speeds, the amount of heat transferred to the workpiece decreases in parallel with increasing chip formation speed [54]. This decrease in tensile residual stresses depending on increase in cutting speed is completely related to decrease in thermal loads in connection with amount of heat transferring to workpiece. As the cutting feed increased, the tensile residual stresses increased as well. This case is parallel with literature [11, 24, 55].

Cutting feed has a strong influence on the shape of the residual stress profile. As the cutting feed increases, rising chip cross-section area increases cutting forces. Due to the fact that higher cutting feeds lead to increase in cutting forces, the energy needed increases as well. The case mentioned above led to increases in tensile residual stresses on the surface together with increasing heat and mechanical loads because the increase in cutting feed for plastic deformation will increase the energy amount needed, and this energy will come out as thermal energy (Figs. 4 and 5). When the graphics in Figs. 4 and 5 are examined, it can be seen that as the depth of cut increases, tensile residual stresses increase as well. However, this influence was not as clear as cutting speed and cutting feed. When looking at the literature, it is possible to see similar results [56–58]. Depending on change of cutting insert rake face forms, the lowest tensile residual stresses were obtained with cutting tools with the form of QM-MM-MR, respectively, when the residual stress graphics obtained were examined (Figs. 4 and 5). The rake angle is the most important factor effecting chip removable process. With the increase in rake angle, tensile residual stresses also decreased. The case in question has the same tendency with the studies carried out by other researchers [23, 48]. As the rake angle increases, shear angle increases as well [34–36]. When the shear angle increases, the temperature occurring on shear plane decreases since plastic deformation of metal occurs on a shorter shear plane. Since this will cause the amount of heat transmitted to workpiece to decrease, this will leave a lower thermal effect on the surface of the workpiece and be resulted with decrease in tensile residual stresses. The small rake angle, by decreasing shear plane angle, increases cutting forces, while the large rake angle, by increasing shear plane angle, decreases cutting forces. Also, one of the most significant factors effecting cutting forces during chip removal is the tool/chip contact length. As rake angle increases, by decreasing of tool/chip contact length and friction force, cutting forces decrease; on the other hand, as rake angle decreases, depending on increase in the tool/chip contact length and friction force, cutting forces increase [36, 59]. Increasing shear angles which are caused by

Fig. 4 Change of circumferential residual stress values (MPa) depending on cutting insert rake face forms and cutting parameters **a** f = 0.1 mm/rev, **b** f = 0.2 mm/rev, and **c** f = 0.3 mm/rev
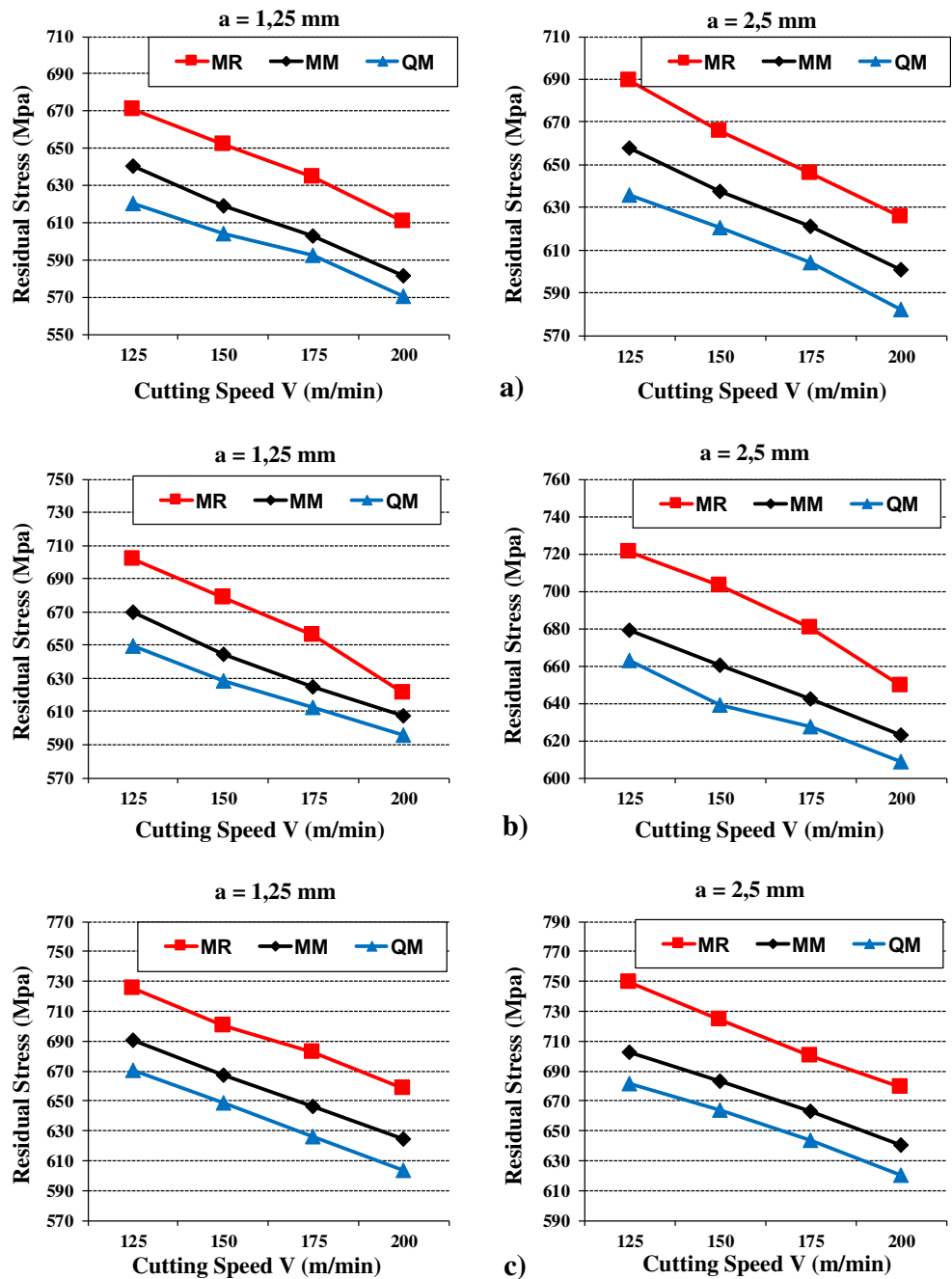

big rake angles in positive direction decreases the tool/contact area, friction force, cutting forces, and heat occurrence. This decreasing heat with mechanical loads will cause to decrease tensile residual stresses occurring on the surface of workpiece.

When the insert rake angles of cutting tools used in experiments are assessed in order of sizes, because of QM(13°)-MM(9°)-MR(6°), the lowest tensile residual stresses occurred on the surfaces machined with cutting tools having QM-MM-MR forms, respectively. This case is clearly seen in the graphics of Figs. 4 and 5. Besides, when evaluated MR-MM-QM formed cutting tools in Fig. 3, it is seen that, respectively, MR(0.33)-MM(0.30)-

QM(0.12) have the highest flat of the insert rake face. Bigger flat of the insert rake face increases tool/chip contact area, while smaller flat of the insert rake face decreases tool/chip contact area. This decreasing too/chip contact length contributes cutting forces and heat occurrence to decrease. Decreasing temperature and cutting forces will decrease thermal and mechanical effect on workpiece, which will cause the decrease of tensile residual stresses. Therefore, the lowest tensile residual stresses occurred on surfaces machined by cutting tools with QM forms and the highest tensile residual stresses on surfaces machined by cutting tools with MR forms. In three

Fig. 5 Change of axial residual stress values (MPa) depending on cutting insert rake face forms and cutting parameters **a** f = 0.1 mm/rev, **b** f = 0.2 mm/rev, and **c** f = 0.3 mm/rev
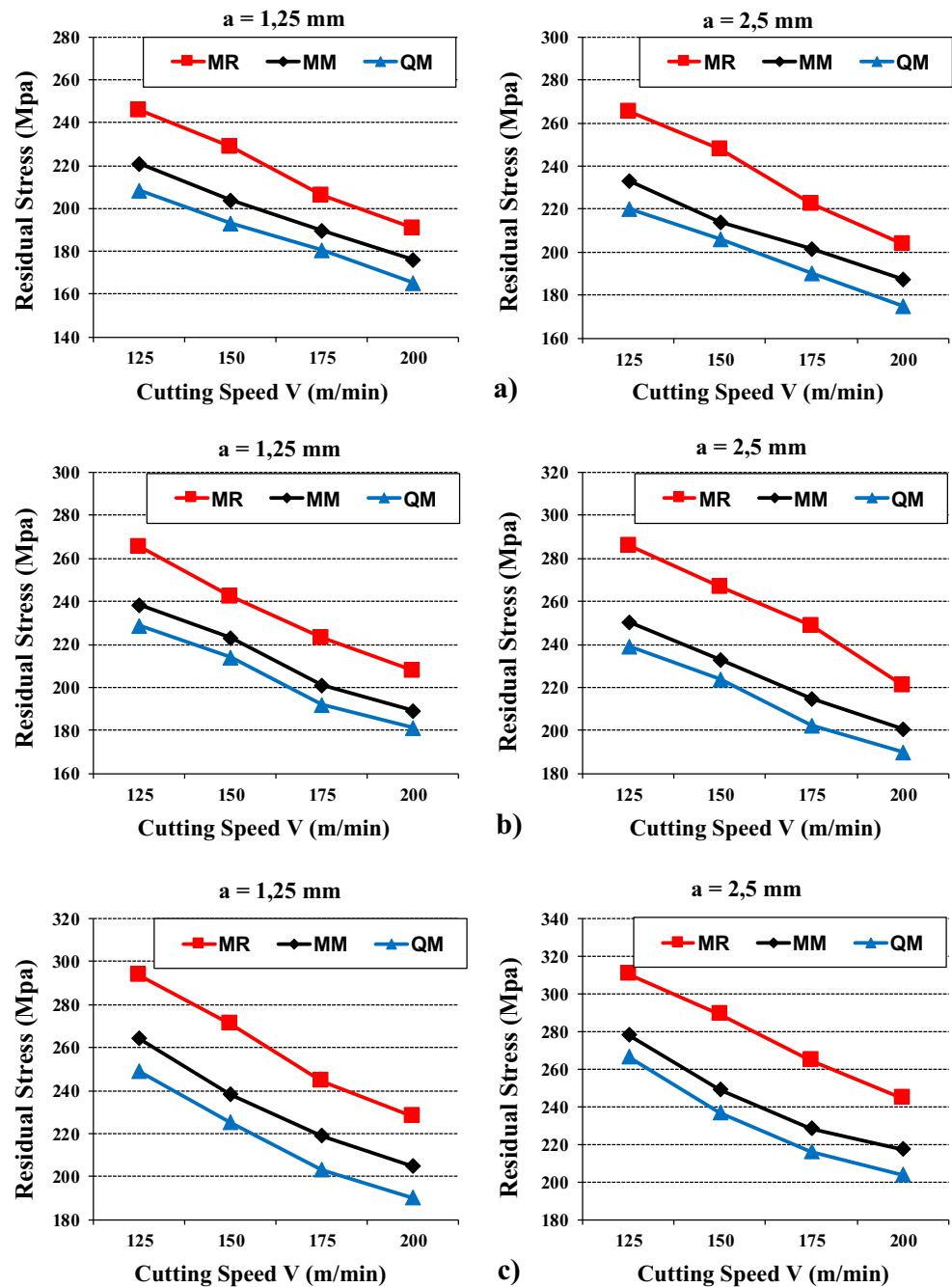

different forms of the tool rake face, the lowest tensile residual stresses were obtained when cutting speed was 200 m/min, cutting feed was 0.1 mm/rev, and depth of cut was 1.25 mm, and the highest tensile residual stresses were obtained when cutting speed was 125 m/min, cutting feed was 0.3 mm/rev, and depth of cut was 2.5 mm.

4.4 Microstructure analysis

The workpieces machined with cutting parameters in V = 125 m/min, f = 0.3 mm/rev, and a = 2.5 mm, where values

of cutting forces and residual stresses were the highest, were selected to see the microstructure change occurring beneath the machined surface. The microstructure changes occurring beneath the machined surface are shown in Fig. 6 depending on form of the cutting insert rake face and determined cutting parameters. When SEM images in Fig. 6 are examined, it is noticed that there is a region beneath the machined surface affected by deformation. Similar results emerged in previous studies on the subject [4–6, 60, 62]. When microstructural changes occurred beneath the machined surface (Fig. 6), the lowest deformation amount occurring beneath the machined

Fig. 6 Microstructural changes beneath machined surface depending on cutting insert rake face forms in cutting parameters $V = 125$ m/dak, $f = 0.3$ mm/dev, and $a = 2.5$ mm, **a** QM form, **b** MM form, and **c** MR form

a) QM Form

b) MM Form

c) MR Form
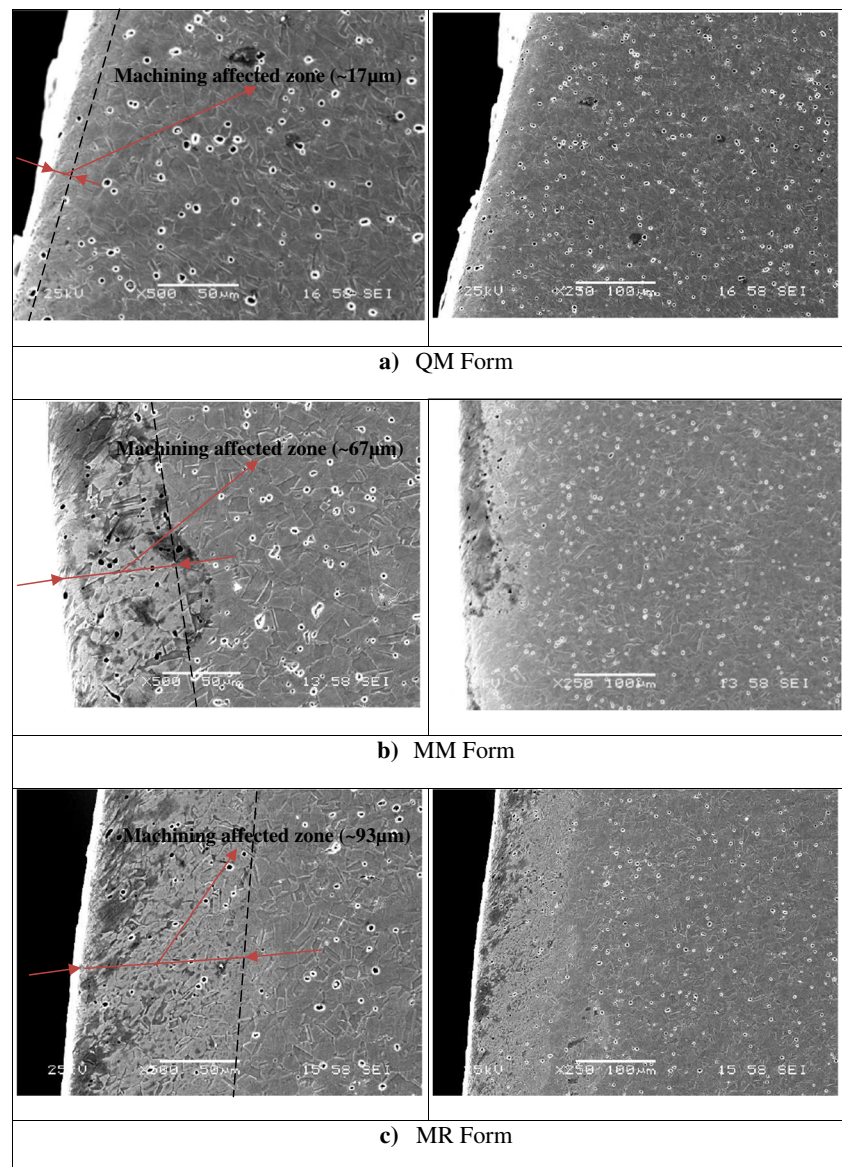
surface were obtained with cutting tools having forms QM (~17 μm)-MM(~67 μm)-MR (~93 μm), respectively. The shear angle is also directly related to the cutting tool rake angle. In some studies taking part in the literature, it was stated that with increase in rake angle, the shear angle also increased [34–36]. With decrease of rake angle or with increase of it in negative direction, shear angle was observed to decrease [34–36]. When shear angle increases, due to the occurrence of plastic deformation of metal on a shorter shear plane, the occurring heat decreases as a result of less energy usage for cutting process on shear plane. Since this will lead to decrease in heat transferred to workpiece, it will cause to decrease in the area affected by deformation with decrease in thermal loads leaving lower thermal effect on workpiece.

Moreover, as the rake angle increases together with decrease in tool/chip contact length and friction force, the cutting

forces decrease; as the rake angle decreases, cutting forces increase depending on tool/chip contact length and increase in friction force [36, 59]. The increasing shear angle depending on big rake angles in positive direction decreases the tool/contact area, friction force, cutting forces, and heat formation. And, this will decrease the amount of deformation beneath the machined surface with the decrease in both thermal and mechanical effects in the plastic deformation process. Depending on size of insert rake angles belonging to cutting tools used in experiments, when the cutting tools with QM(13°)-MM(9°)-MR(6°) were arranged, the area least affected by deformation occurred beneath the surfaces machined with cutting tools having QM-MM-MR forms, respectively. This case can be clearly seen in comparative pictures (Fig. 6). That the least deformation amount occurring beneath the machined surface was obtained with cutting tools having

the forms QM(~17 μm)-MM(~67 μm)-MR(~93 μm), respectively, and that mechanical loads constituted a non-homogenous deformed plastic layer beneath the machined surface was associated with it.

When we look at the cutting forces obtained with cutting tools having these three types of forms (MR-MM-QM) (Fig. 2), while the lowest cutting forces were obtained with cutting tool with QM (13°) form having the highest insert rake angle, we find that the highest cutting forces were obtained with cutting tool with MR (6°) having the lowest insert rake angle. As a result, it is thought that increase or decrease in mechanical loads lead to increase or decrease in the area affected by deformation. At the same time, when examined cutting tools have forms of MR-MM-QM in Fig. 3, it was seen that they have the biggest flat of the insert rake face MR(0.33)-MM(0.30)-QM(0.12), respectively. While bigger flat of the insert rake face increases tool/chip contact area, smaller flat of the insert rake face decreases tool/chip contact area. The decreasing tool/chip contact length helps cutting forces and heat formation to decrease. The decreasing temperature and cutting forces will lead to the decrease of the area affected from deformation by reducing the thermal and mechanical effects on the workpiece.

4.5 Microhardness measurement

At the end of the test results, the changes in microhardness values measured depending on applied cutting parameters and forms of the cutting insert rake face are shown in graphics in Fig. 7. When the graphics in Fig. 7 are examined, for all machining experiments, immediately beneath the machined surface when progressed from deformed material toward not having deformed (bulk material), it was observed that microhardness values decreased and the material reached to its average hardness values (202 ± 3). The same tendency was seen in the studies about the issue [4–6, 61–65]. The researchers emphasized that the reason for obtaining the highest hardness in the region closest to the machined surface, after machining, was due to work hardening depending on plastic deformation [4, 5, 63, 65, 66]. In literature, it was stated that a work-hardening layer could be formed easily as response to the machining which the deformations beneath the machined surface caused [63].

When the microhardness values graphics in Fig. 7 were examined, it was seen that the lowest microhardness values were found to be below those of the surfaces machined with cutting tools having insert rake angles QM (13°)-MM(9°)-MR(6°), respectively. The highest microhardness values were obtained with the cutting tools with MR(6°) form which had the lowest insert rake angle; the lowest microhardness values were obtained with cutting tools with QM (13°) form which

had the highest insert rake angle beneath the machined surfaces. Together with increase in rake angle, microhardness values decreased. As the rake angle increases, shear angle increases as well [34–36]. When shear angle increases, the heat occurring on the shear plane decreases because plastic deformation of metal is realized along shorter shear surface. While small rake angle increases cutting forces by decreasing shear plane angle, big rake angle decreases the cutting forces by increasing shear plane angle. Increase in rake angle decreases with decreasing of tool/chip contact length and friction forces, and the cutting forces also decrease [36, 59]. Increasing of shear angle due to big rake angles in positive direction decreases the tool/chip contact area, cutting forces, and heat occurrence.

As mentioned above, increase in rake angle and decrease in thermal and mechanical loads during plastic deformation will lead to decrease in area affected from deformation beneath the machined surface of workpiece. At the same time, when looking into cutting tools with the form of MR-MM-QM in Table 2, it is seen that the biggest flat of the insert rake face is possessed by MR(0.33)-MM(0.30)-QM(0.12), respectively. While bigger flat of the insert rake face increases the tool/chip contact area, smaller flat of the insert rake face decreases the tool/chip contact area. This decreasing tool/chip contact length helps cutting forces and heat occurrence to decrease. The decreasing heat and cutting forces lead to decrease in the area affected from deformation decreasing thermal and mechanical effects on the surface of workpiece. The lowest microhardness values are seen beneath the machined surface by cutting tools with the form of QM(~17 μm)-MM(~67 μm)-MR(~93 μm) causing the least deformation beneath the machined surface, respectively (Fig. 6). In his studies, Che-Haron stated that he obtained the highest microhardness values beneath the machined surface, where microstructure was heavily deformed, and the lowest microhardness values beneath the machined surface, where microstructure was lightly deformed [4, 5].

In the experiments conducted, it is observed that, in general, when depth of cut and cutting feed increase, microhardness values increase; however, microhardness values decrease with increase in cutting speed (Fig. 7). As cutting speed increased, microhardness values decreased. Similar results were shown in the studies carried out by Pawade and Bosheh during machining of Inconel 718 and H13 tool steels, obtaining high microhardness values at low cutting speeds [64, 65]. In literature, it is stated that cutting speed has a significant effect on heat occurrence during machining [65]. The cutting speed rate defines the necessary energy to remove the chip; therefore, it is directly related to heat amount occurring during cutting process. During machining, about 10–15 % of heat occurrence are transferred to workpiece. When machining is carried out at high cutting
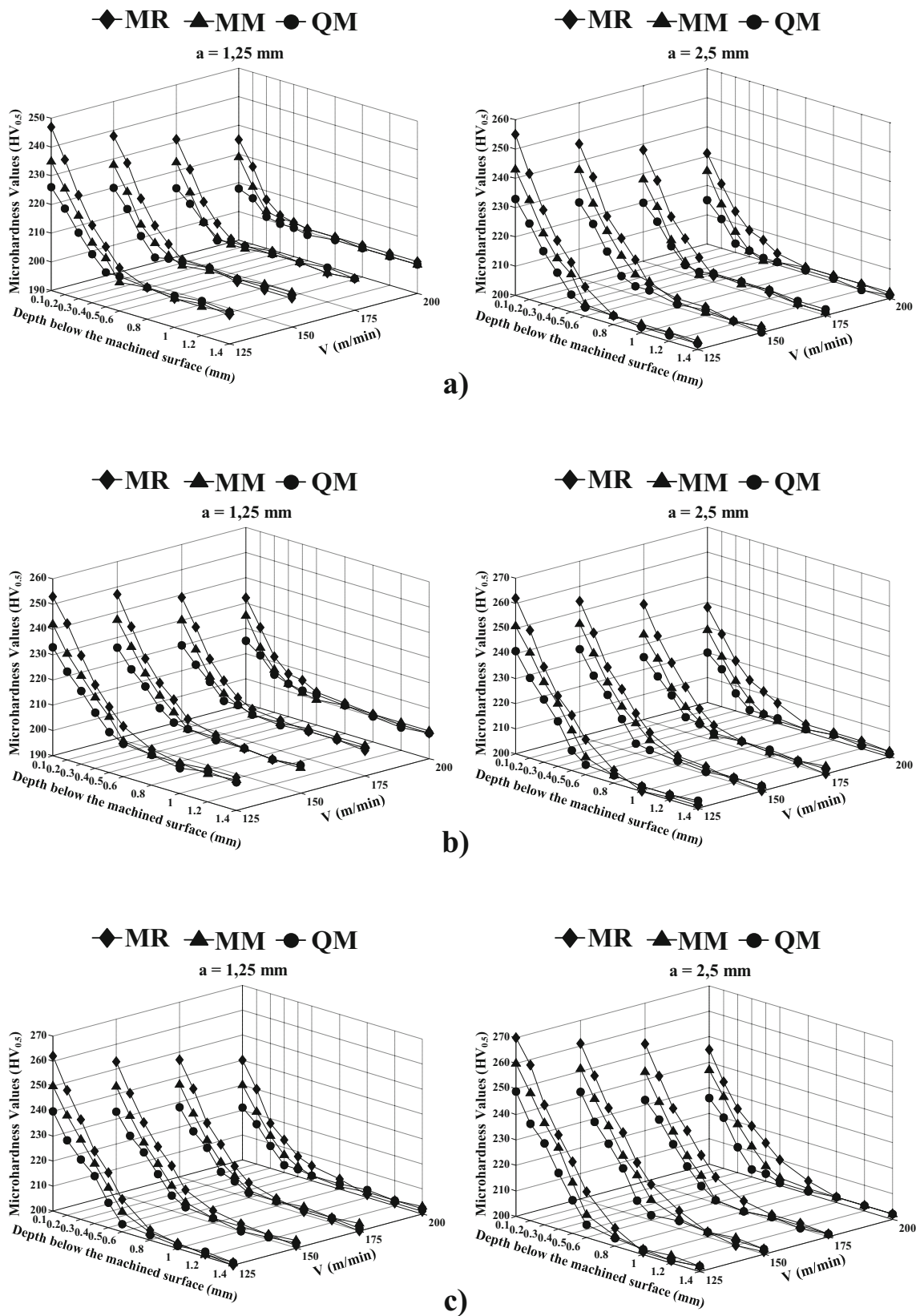
Fig. 7 Change of microhardness values (HV0.5) depending on cutting insert rake face forms and cutting parameters **a** f = 0.1 mm/rev, **b** f = 0.2 mm/rev, and **c** f = 0.3 mm/rev

speeds, the heat transferring to the workpiece decreases [54]. Therefore, since increase in cutting speed will cause heat amount transferring to workpiece to decrease, this can lead to low microhardness values in surface layer.

When the microhardness graphics in Fig. 7 are examined, it can be seen that as the depth of cut and cutting feed increased and microhardness values also increased. When looking at literature, it is possible to see similar results [61, 67]. As the cutting feed and depth of cut increase, chip cross section increases as well. Due to the fact that higher cutting feed causes increase in cutting forces, this will increase the energy amount necessary for plastic deformation. Since this increasing energy will come out in the form of thermal energy, together with high thermal and mechanical loads, it causes increase in higher microhardness values in the deformed area immediately beneath the machined surface (Fig. 7).

5 Conclusions

It is proven experimentally that the shape of the rake face of the cutting insert has significant influence on its performance in terms of the cutting force and integrity of the machined surface. According to Astakhov and Xiao [19], it happens because the shapes of the rake face affect the state of stress in the deformation zone, particularly the stress triaxiality state. As a result, the energy needed at the zone of separation of the chip and workpiece is altered by the shape of the rake face. As this energy affects both the chip and the machined surface, the changes in the cutting force for different shapes occur in parallel with machined surface integrity. Therefore, the selection of the shape of the rake face should be carried out not only using the shape of the formed chip as a criterion but also should include considerations of the cutting force and machined surface integrity.

In this study, the following summarized results are attained after evaluating the findings obtained depending on forms of tool rake face and cutting parameters in machining of AISI 316 L austenitic stainless steel.

- The best surface integrity results were obtained with cutting tools with QM form, while the worst surface integrity results were obtained with cutting tools with MR form.
- It was figured out that forms of cutting insert rake face and cutting parameters had a significant effect on surface integrity.
- In the experiments conducted, in general, it was observed that when depth of cut and cutting feed were increased, surface integrity values also increased; however, when the cutting speed was increased, surface integrity values decreased.

- In all experiments, it occurred that the effect of cutting feed on surface roughness was more effective than cutting speed and depth of cut; however, the effect of cutting speed and cutting feed on tensile residual stresses was more effective than depth of cut.
- The lowest tensile residual stresses (circumferential and axial) were obtained from surfaces machined with cutting tools with forms of QM-MM-MR forms, respectively.
- The least deformation amount occurring beneath the machined surface was obtained by cutting tools having forms of QM (~17 μm)-MM(~67 μm)-MR (~93 μm), respectively, while the lowest microhardness values were obtained beneath the machined surface with cutting tools, which causes the least deformation, having forms of QM-MM-MR, respectively.
- The best surface integrity turned out when cutting speed was 200 m/min, cutting feed was 0.1 mm/rev, and depth of cut was 1.25 mm, while the worst surface integrity turned out when surface cutting speed was 125 m/min, cutting feed was 0.3 mm/rev, and depth of cut was 2.5 mm.

References

1. Arunachalam RM, Manan MA, Spowage AC (2004) Surface integrity when machining age hardened Inconel 718 with coated carbide cutting tools. Int J Mach Tools Manuf 44:1481–1491

2. Chou YK (2002) Surface hardening of AISI 4340 steel by machining: a preliminary investigation. J Mater Process Technol 124:171–177

3. Alexander D, Bernardo L, David J, Escobar Maria D (2010) Effect of the variation of cutting parameters in surface integrity in turning processing of an AISI 304 austenitic stainless steel. Technical contribution to the First International Brazilian Conference on Tribology, Brazil 434–446

4. Che-Haron CH (2001) Tool life and surface integrity in turning titanium alloy. J Mater Process Technol 118:231–237

5. Che-Haron CH, Jawaid A (2005) The effect of machining on surface integrity of titanium alloy Ti–6%Al–4%V. J Mater Process Technol 166:188–192

6. Devillez A, Coz GL, Dominiak S, Dudzinski D (2011) Dry machining of Inconel 718 workpiece surface integrity. J Mater Process Technol 211:1590–1598

7. Sharman ARC, Hughes JI, Ridgway K (2015) The effect of tool nose radius on surface integrity and residual stresses when turning Inconel 718. J Mater Process Technol 216:123–132

8. Bordin A, Bruschi S, Ghiotti A (2014) The effect of cutting speed and cutting feed on the surface integrity in dry turning of CoCrMo alloy. 2nd CIRP conference on surface integrity (CSI). Procedia CIRP 13:219–224

9. Jacobson M, Dahlman P, Gunnberg F (2002) Cutting speed influence on surface integrity of hard turned bainite steel. J Mater Process Technol 128:318–323

10. Rech J, Moisan A (2003) Surface integrity in finish hard turning of case hardened steels. Int J Mach Tools Manuf 43(5):543–550

11. Matsumoto Y, Hashimoto F, Lahoti G (1999) Surface integrity generated by precision hard turning. Annals of the CIRP 48(1):59–62

12. El-Wardany TI, Kishawy HA, Elbestawi MA (2000) Surface integrity of die material in high speed hard machining, part 1: Micrographical analysis. ASME J Manuf Sci And Eng 122:620–631

13. Kishawy HA, Elbestawi MA (2001) Tool wear and surface integrity during high-speed turning of hardened steel with polycrystalline cubic boron nitride tools. J Eng Manuf 215:755–767

14. Schwach DW, Guo YB (2005) Feasibility of producing optimal surface integrity by process design in hard turning. Mater Sci Eng A 395(1–2):116–123

15. Smith S, Melkote SN, Lara-Curzio E, Watkins TR, Allard L, Riester L (2007) Effect of surface integrity of hard turned AISI 52100 steel on fatigue performance. Mater Sci Eng A 459:337–346

16. Shi J, Liu Richard C (2010) Two-step cutting for improving surface integrity and rolling contact fatigue performance of hard machined surfaces. Mater Manuf Process 25:495–502

17. Gurbuz H, Kafkas F, Seker U (2012) The effect of tool cutting edge form chip breaker forms on cutting forces and surface roughness in machining AISI 316 L steel. J Life Sci 1(2):173–184

18. Gurbuz, H (2012) Investigation of the effects of cutting tool geometry and coating types on surface integrity in machining of AISI 316 L steel. Ph.D. Thesis, Gazi Universty, Turkey, 1–179

19. Astakhov VP, Xiao X (2016) The principle of minimum strain energy to fracture of the work material and its application in modern cutting technologies. Chapter 1 in book: Davim JP (ed) Metal Cutting Technologies, Progress and Current Trends; pp. 1–35

20. Sandvik Coromant, (2010) Sipariş Katoloğu-Sandvik Coromanttan Kesici Takımlar 2009, C-2900:8 AB Sandvik Coromant. İsveç, A123

21. Sandvik Coromant, (2010) Teknik Kılavuz, C-2900:7 AB Sandvik Coromant, İsveç A101. 103–105, H12

22. Outeiro JC, Dias AM, Jawahir IS (2006) On the effects of residual stresses induced by coated and uncoated cutting tools with finite edge radii in turning operations. Ann CIRP 55(1):111–116

23. Outeiro JC, Dias AM, Lebrun JL, Astakhov V (2002) Machining residual stresses in AISI 316 L steel and their correlation with the cutting parameters. Mach Sci Technol 6(2):251–270

24. M'Saoubi R, Outeiro JC, Changeux B, Lebrun JL, Moraäo Dias A (1999) Residual stress analysis in orthogonal machining of standard and resulfurized AISI 316 L steels. J Mater Process Technol 96:225–233

25. Outeiro JC, Pina JC, M'Saoubi R, Pusavec F, Jawahir IS (2008) Analysis of residual stresses induced by dry turning of difficult-to-machine materials. CIRP Ann-Manufac Technol 57:77–80

26. Cullity BD (1978) Elements of X-ray diffraction 2nd ed. Addison-Wesley Series in Metallurgy and Materials Canada 86-87:460–461

27. Chen W (2000) Cutting forces and surface finish when machining medium hardness steel using CBN tools. Int J Mach Tools Manuf 40:455–466

28. Zhao J, Ai X, Li Z (2006) Finite element analysis of cutting forces in high speed machining. Mater Sci Forum 532-533:753–756

29. Trent EM (1989) Metal cutting. Butterworths Press, London, pp. 1–171

30. Çiftçi İ (2006) Machining of austenitic stainless steels using CVD multi-layer coated cemented carbide tools. Tribol Int 39:565–569

31. Suresh R, Basavarajappa S, Samuel GL (2012) Some studies on hard turning of AISI 4340 steel using multilayer coated carbide tool. Measurement 45:1872–1884

32. Shoba C, Ramanaiah N, Nageswara Rao D (2015) Effect of reinforcement on the cutting forces while machining metal matrix compositese an experimental approach. Engineering science and technology an. Int J 18:658–663

33. Marinov VR (2001) Hybrid analytical-numerical solution for the shear angle in orthogonal metal cutting—part II: experimental verification. Int J Mech Sci 43:415–426

34. Shih AJ (1996) Finite element analysis of the rake angle effects in orthogonal cutting. Int J Mech Sci 38(1):1–17

35. Moufki A, Molinari A, Dudzinski D (1998) Modelling of orthogonal cutting with a temperature dependent friction law. J Mech Phys Solids 46:2103–2138

36. Saglam H, Unsacar F, Yaldiz S (2006) Investigation of the effect of rake angle and approaching angle on main cutting force and tool tip temperature. Int J Mach Tools Manufac 46:132–141

37. Shaw MC (1989) Metal cutting principles. Oxford University Press, Oxford, pp. 1–9

38. De Garmo EP, Black JT, Kohser RA (1997) Materials and processes in manufacturing. Prentice-Hall Inc., New Jersey, pp. 214–652

39. Boothroyd G (1989) Fundamentals of metal machining and machine tools, Second edn. McGraw-Hill, New York, pp. 166–172

40. Munoz–Escalona P, Cassier Z (1998) Influence of the critical cutting speed on the surface finish of turned steel. Wear 218:103–109

41. Thamizhmanii S, Kamarudin KE, Rahim A, Saparudin A, Hassan S (2007) Tool wear and surface roughness in turning AISI 8620 using coated ceramic tool. Proceedings of the World Congress on Engineering, Vol II WCE, London, pp. 1157–1161

42. Gupta M, Kumar S (2015) Investigation of surface roughness and MRR for turning of UD-GFRP using PCA and Taguchi method. Eng Sci Technol Int J 18:70–81

43. Suresh R, Basavarajappa S (2014) Effect of process parameters on tool wear and surface roughness during turning oj hardened steel with coated ceramic tool. Procedia Mater Sci 5:1450–1459

44. Nasr MNA, Ng EG, Elbestawia MA (2008) A modified time-efficient FE approach for predicting machining-induced residual stresses. Finite Elem Anal Des 44:149–161

45. Valiorgue F, Rech J, Hamdi H, Gilles P, Bergheau JM (2007) A new approach for the modelling of residual stresses induced by turning of 316L. J Mater Process Technol 191:270–273

46. Ee KC, Dillon OW, Jawahir IS (2005) Finite element modeling of residual stresses in machining induced by cutting using a tool with finite edge radius. Int J Mech Sci 47:1611–1628

47. Liang SY, Su JC (2007) Residual stress modeling in orthogonal machining. Annals of the CIRP 56(1):65–68

48. Outeiro JC, Umbrello D, M'Saoubi R (2006) Experimental and numerical modelling of the residual stresses induced in orthogonal cutting of AISI 316 L steel. Int J Mach Tools Manufac 46(14):1786–1794

49. Ulutan D, Alaca BE, Lazoglu I (2007) Analytical modelling of residual stresses in machining. J Mater Process Technol 183:77–87

50. Mohammadpour M, Razfar MR, Saffar JR (2010) Numerical investigating the effect of machining parameters on residual stresses in orthogonal cutting. Simul Model Pract Theory 18:378–389

51. Maranhão C, Davim PJ (2010) Finite element modelling of machining of AISI 316 steel: numerical simulation and experimental validation. Simul Model Pract Theory 18:139–156

52. Kishawy HEA, (1998) Chip formation and surface integrity in high speed machining of hardened steel. Doctor of Philosophy, Mc Master University; Canada, 87–89

53. Liu CR, Barash MM (1982) Variables governing patterns of mechanical residual stress in a machined surface. J Eng Ind Trans ASME 104(3):257–264

54. Sandvik Coromant (1994) Modern metal cutting—a practical handbook . Sandvik Coromant, Sweden, pp. I–IIIEnglish Edition

55. Sharman ARC, Hughes JI, Ridgway K (2006) An analysis of the residual stresses generated in Inconel 718 when turning. J Mater Process Technol 173:359–367

56. Dahlman P, Gunnberg F, Jacobson M (2004) The influence of rake angle, cutting feed and cutting depth on residual stresses in hard turning. J Mater Process Technol 147:181–184

57. Sasahara H, Obikawa T, Shirakashi T (2004) Prediction model of surface residual stress within a machined surface by combining two orthogonal plane models. Int J Mach Tools Manufac 44:815–822

58. Gunnberg F, Escursell M, Jacobson M (2006) The influence of cutting parameters on residual stresses and surface topography during hard turning of 18MnCr5 case carburised steel. J Mater Process Technol 174:82–90

59. Günay M, Korkut İ, Aslan E, Şeker U (2005) Experimental investigation of the effect of cutting tool rake angle on main cutting force. J Mater Process Technol 166:44–49

60. Javidi A, Rieger U, Eichlseder W (2008) The effect of machining on the surface integrity and fatigue life (technical note). Int J Fatigue 30:2050–2055

61. Ezugwu EO, Wang ZM, Okeke CI (1999) Tool life and surface integrity when machining Inconel 718 with PVD and CVD coated tools. Tribol Trans 42(2):353–360

62. Sharman ARC, Hughes JI, Ridgway K (2004) Workpiece surface integrity and tool life issues when turning Inconel 718 nickel based superalloy. Mach Sci Technol 8(3):399–414

63. Ulutan D, Ozel T (2011) Machining induced surface integrity in titanium and nickel alloys: a review. Int J Mach Tools Manuf 51:250–280

64. Bosheh SS, Mativenga PT (2006) White layer formation in hard turning of H13 tool steel at high cutting speeds using CBN tooling. Int J Mach Tools Manuf 46:225–233

65. Pawade RS, Joshi SS, Brahmankar PK (2008) Effect of machining parameters and cutting edge geometry on surface integrity of high-speed turned Inconel 718. Int J Mach Tools Manuf 48:15–28

66. Coelho RT, Silva LR, Braghini A Jr, Bezerra AA (2004) Some effects of cutting edge preparation and geometric modifications when turning Inconel 718 at high cutting speeds. J Mater Process Technol 148(1):147–153

67. Umbrello D, Filice L (2009) Improving surface integrity in orthogonal machining of hardened AISI 52100 steel by modeling white and dark layers formation. CIRP Ann Manufact Technol 58:73–76